These numbers are within a factor of two of those observed here. Given the experimental uncertainties of the parameters used in the calculations, and the simplicity of the model used (a single pair of parallel, Gaussian vortices), this approximate agreement is encouraging. Higher resolution PIV data could directly confirm or deny the presence of the elliptic mode in these vortices, by showing if the core and the periphery were displaced relative to each other. An elliptic instability was in fact demonstrated this way by Leweke and Williamson[15] for an equal-strength counter-rotating pair at $Re_\Gamma \approx 3 \times 10^3$.

Conclusions

Corotating tip–flap vortex pairs are studied at Re_Γ of order 10^5. The evolution of the velocity field at a fixed cross section is recorded, yielding measures of the circulation ratio, separation, and vortex size. The pair is observed to merge within about one orbital period. Flow visualization clearly shows the three-dimensional nature of this process, with the appearance of strong sinuous disturbances on the weaker flap vortex, and to a lesser extent on the tip vortex. The wave number of this disturbance and its alignment with the extensional axis of the straining field from the partner vortex suggest it to be an example of an elliptical instability. For such an instability driven by the straining field of the partner vortex, the growth rate scales as the inverse of the square of the vortex separation, $1/d^2$. This growth rate matches the scaling of the orbit period, thus, yielding finite amplitudes within one orbit. This provides an explanation for the observed merger in about one orbit, even for vortices spaced too far apart to merge in two dimensions.

Acknowledgments

R. L. Bristol and J. M. Ortega acknowledge the support of the National Science Foundation Graduate Fellowship program during the course of this research.

References

[1]Donaldson, C., and Bilanin, A., "Vortex Wakes of Conventional Aircraft," AGARDograph 204, edited by R. H. Korkegi, May 1975.

[2]Rossow, V. J., "Lift-Generated Vortex Wakes of Subsonic Transport Aircraft," *Progress in Aerospace Sciences*, Vol. 35, No. 6, 1999, pp. 507–660.

[3]Ciffone, D., and Lonzo, C., "Flow Visualization of Vortex Interactions in Multiple Vortex Wakes Behind Aircraft," NASA TM X-62, 459, June 1975.

[4]Chen, A. L., Jacob, J. D., and Savaş, Ö., "Dynamics of Corotating Vortex Pairs in the Wakes of Flapped Airfoils," *Journal of Fluid Mechanics*, Vol. 382, 1999, pp. 155–193.

[5]Bristol, R. L., Ortega, J. M., and Savaş, Ö., "A Towing Tank Study of Airfoil Wake Vortices at Re_Γ of Order 10^5," AIAA Paper 99-3419, June 1999.

[6]Crow, S. J., "Stability Theory for a Pair of Trailing Vortices," *AIAA Journal*, Vol. 8, No. 12, 1970, pp. 2172–2179.

[7]Jimenez, J., "Stability of a Pair of Co-Rotating Vortices," *Physics of Fluids*, Vol. 18, No. 11, 1975, pp. 1580–1581.

[8]Klein, R., Majda, A. J., and Damodaran, K., "Simplified Equations for the Interaction of Nearly Parallel Vortex Filaments," *Journal of Fluid Mechanics*, Vol. 288, 1995, pp. 201–248.

[9]Crouch, J. D., "Instability and Transient Growth for Two Trailing-Vortex Pairs," *Journal of Fluid Mechanics*, Vol. 350, 1997, pp. 311–330.

[10]Bristol, R. L. "Co-operative Wake Vortex Instabilities," Ph.D. Dissertation, Dept. of Physics, Univ. of California, Berkeley, CA, Dec. 2000.

[11]Ortega, J. M., Bristol, R. L., and Savaş, Ö., " Experimental Study of the Instability of Unequal-Strength Counter-Rotating Vortex Pairs," *Journal of Fluid Mechanics*, Vol. 474, 2003, pp. 35–84.

[12]Rossow, V. J., "Convective Merging of Vortex Cores in Lift-Generated Wakes," *Journal of Aircraft*, Vol. 14, No. 3, 1977, pp. 283–290.

[13]Widnall, S. E., Bliss, D., and Tsai, C., "The Stability of Short Waves on a Vortex Ring," *Journal of Fluid Mechanics*, Vol. 66, No. 1, 1974, pp. 35–47.

[14]Eloy, C., and Le Dizes, S., "Three-Dimensional Instability of Burgers and Lamb–Oseen Vortices in a Strain Field," *Journal of Fluid Mechanics*, Vol. 378, 1999, pp. 145–166.

[15]Leweke, T., and Williamson, C. H. K., "Cooperative Elliptic Instability of a Vortex Pair," *Journal of Fluid Mechanics*, Vol. 360, 1998, pp. 85–119.

A. Plotkin
Associate Editor

Reynolds-Number Correlations for Separation of Turbulent Boundary Layers

V. A. Sandborn*
Colorado State University, Fort Collins, Colorado 80521

Introduction

A PHYSICAL model for turbulent boundary-layer separation was proposed by Sandborn and Kline,[1] as a transition region from unseparated to separated flow. Correlations were developed to indicate the onset of intermittent and zero-mean surface shear stress, $\bar{\tau}_w = 0$ separations, in terms of the velocity profile shape factor H and the ratio of displacement to boundary-layer thickness δ^*/δ. The intermittent separation location was taken as the point where the adverse effects associated with flow separation are present and viscous constraints are no longer important. It is the location most researchers identify by flow visualization as turbulent separation, and the point most often predicted by analytical studies. Sandborn and Liu[2] demonstrated that the $\bar{\tau}_w = 0$ separation was equivalent to laminar boundary-layer separations.

The present Note demonstrates that the separation correlations of Sandborn and Kline can be recast in terms of the Reynolds number instead of the less well-defined boundary-layer thickness.

Separation Correlations

Figure 1 shows the curves obtained when the Sandborn–Kline correlations are recast in terms of R_θ. Extrapolated values of form factor and Reynolds number were determined for each set of data points where they crossed the original Sandborn–Kline correlation curves. (See Sandborn and Kline[1] for references to the experimental data.) Most of the variation of H with R_θ occurs for values of R_θ less than 2×10^4. For values of R_θ greater than 2×10^4, the variation of H is quite small ($H \approx 2.5 + 0.2$ for intermittent separation and $H \approx 3.8 + 0.1$ for $\bar{\tau}_w = 0$). The $\bar{\tau}_w = 0$ curve was reported previously.[3]

The compressible flow values (local Mach number ~0.33 and 0.59) of H and R_θ shown on Fig. 1 are the incompressible transformed values (untailed) and the direct, mass flow values (tailed). The compressible measurements were made in a 10×15 cm, cross-section facility at the NASA Ames Research Center (see Sandborn and Seegmiller[4] for details of the basic facility). Details of the tunnel setup for the measurements in the 61×61 cm tunnel were given by Sandborn.[5]

Whereas the separation transition process begins with the first appearance of backflow, the cross-hatched region on Fig. 1 indicates the area where the major adverse problems associated with separation are present. The cross-hatched region corresponds to that part of the flow where the mean flow quantities overshadow the Reynolds turbulent terms.[2]

The fourth-power polynomial (computer fitting), shown in Fig. 1, was employed to estimate the value of the skin-friction coefficient for intermittent separation. Computed values of c_f at the location of intermittent separation are shown on Fig. 2.

To demonstrate the affect of Reynolds number on separation, a set of measurements were made in a small 8.9×16.5 cm inlet duct. The duct was expanded to 25.4 cm ($\delta/R \approx 0.02$) to produce

Received 7 July 2002; revision received 20 November 2002; accepted for publication 30 November 2002.

*Emeritus Professor, Department of Civil Engineering, Engineering Research Center; v.sandborn@attbi.com. Senior Member AIAA.

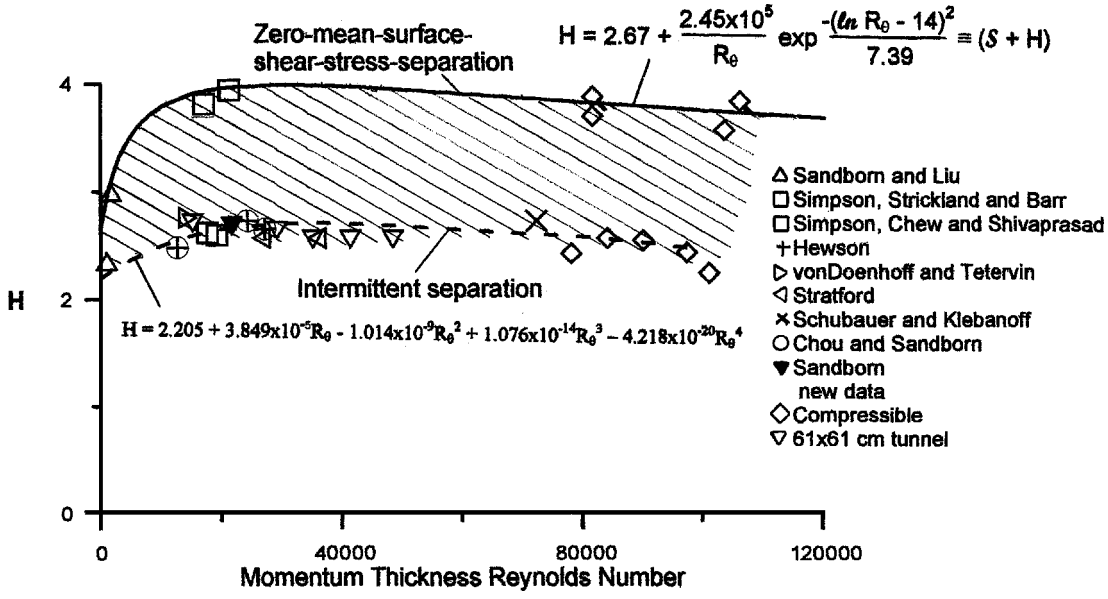

Fig. 1 Turbulent separation correlations in terms of momentum thickness Reynolds number.

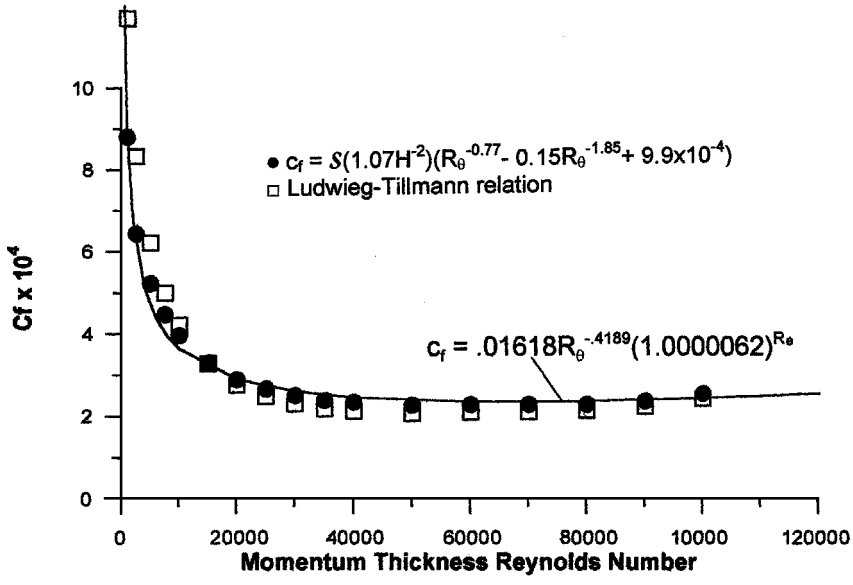

Fig. 2 Estimate of the skin-friction coefficient at intermittent separation.

separation. Figure 3 shows the variation of the shape factor with R_θ for varying inlet velocities. The duct geometry remained the same for all flows; however, boundary-layer growth and the laminar-to-turbulent transition varied slightly from flow to flow. (Note that two blowers powered the facility, which produced slightly different flows in the overlap region around $Re/m \approx 8.2 \times 10^5$.) When the data of Fig. 3 are plotted on the original Sandborn–Kline coordinates, as shown on the insert of Fig. 3, the measurements indicate roughly a single curve. The original Sandborn–Kline correlations can reflect variations of flow geometry and pressure gradient on separation.

Clauser[6] demonstrated experimentally that proper adjustment of the adverse pressure gradient would result in similar or equilibrium turbulent boundary layers. Clauser identified two parameters, which can be related to the Sandborn–Kline coordinates[7]:

$$G = \frac{1}{\Delta}\int_0^\infty \left(\frac{U_e - U}{U_\tau}\right)^2 \mathrm{d}y, \qquad \Delta = \int_0^\infty \frac{U_e - U}{U_\tau}\,\mathrm{d}y$$

$$\text{or} \quad H = \frac{1}{1 + G/(\Delta/\delta)(\delta^*/\delta)} \tag{1}$$

where U_e is the freestream velocity and U_τ is the shear-stress velocity. The ratio $G/(\Delta/\delta)$ maintained constant produced the equilibrium turbulent boundary-layer profiles. Figure 4 (Refs. 2 and 8–10) is a plot of Eq. (1) for a number of values of $G/(\Delta/\delta)$. These curves might be viewed as demonstrating the effect of pressure gradient related to separation. The Sandborn–Kline correlations are also shown in Fig. 4.

The experimental points shown on Fig. 4 were not equilibrium cases; however, they demonstrate the range of values of $G/(\Delta/\delta)$ necessary to include the different types of flows. The flow of Simpson et al.[8] [$G/(\Delta/\delta) \approx 1.45$ to 1.5] was along a "flat plate" with an imposed pressure gradient ($\delta/R < 0.01$, where R is the radius of curvature). The curvature case of Sandborn and Liu[2] corresponds to $G/(\Delta/\delta) \approx 2.75(\delta/R \approx 0.13)$. The direct connection between curvature and pressure gradient makes it difficult to isolate the two effects.

Representation of the velocity distribution in turbulent boundary layers employ almost exclusively Coles's[9] law-of-the-wall–law-of-the-wake empirical profile(s). This approach requires that all turbulent boundary-layer separation be reduced to a single profile for the case of $\bar{\tau}_w = 0$. The analysis of Kline et al.[11] demonstrated that Coles's velocity distributions belong to one equilibrium flow family, with slight Reynolds-number variations for zero and small pressure gradients. Curve(s) of H vs δ^*/δ given by Kline et al.,[11] as obtained for Coles's profile(s) are shown on Fig. 4. These curves correspond

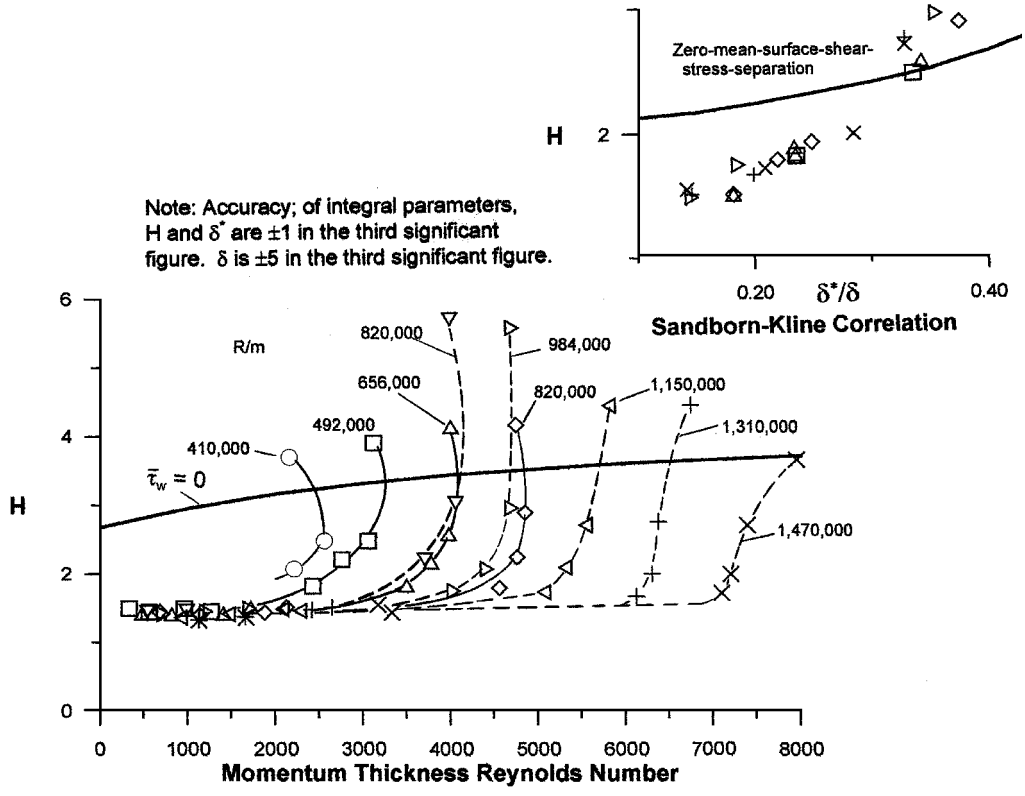

Fig. 3 Separation measurements in the 8.9 × 16.5 cm tunnel.

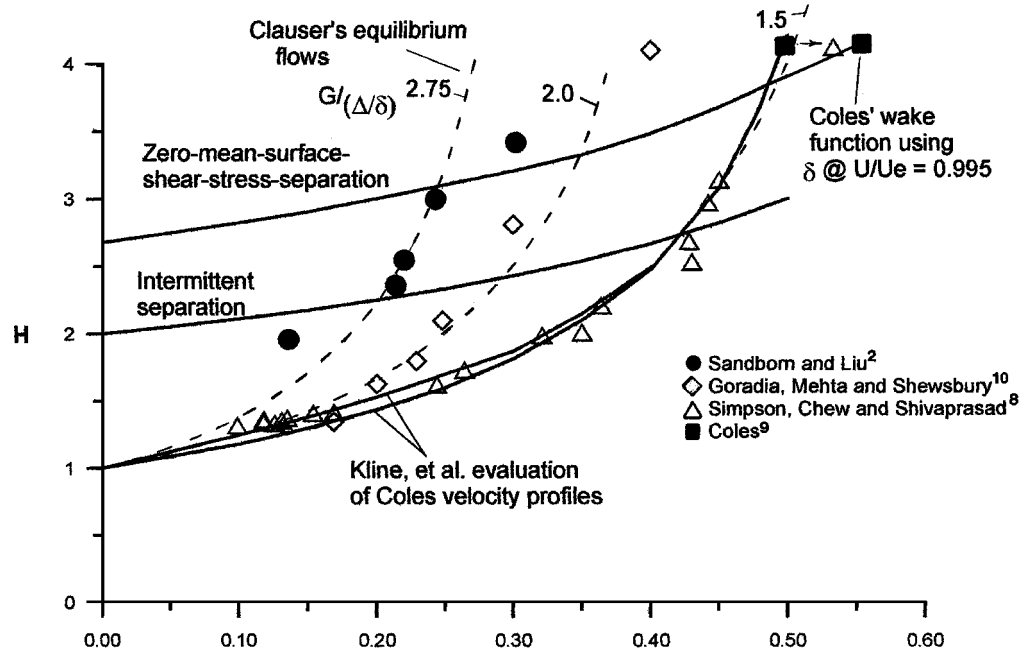

Fig. 4 Sandborn–Kline separation correlations compared to measurements and equilibrium flows.

roughly to the Clauser curve for $G/(\Delta/\delta) \approx 1.5$. If the boundary-layer thickness of Coles's wake function is taken at the point where $U/U_e = 0.995$, then the wake function parameters are $\delta^*/\delta = 0.541$ and $H = 4.19$, which fall directly on the $\bar{\tau}_w = 0$ Sandborn–Kline correlation. Thus, Coles's tabulated wake function is just one profile of the general empirical profile necessary to represent the spectrum of separations.

Conclusions

The present analysis employs information from a number of new and existing experimental turbulent boundary-layer separation studies to recast the Sandborn–Kline separation correlations in terms of velocity shape factor and momentum thickness Reynolds number. The original correlations in terms of shape factor and the ratio of displacement to boundary-layer thickness appear to reflect the effects of pressure gradient and curvature on separation; however, it was not possible to separate these variables.

References

[1]Sandborn, V. A., and Kline, S. J., "Flow Models in Boundary Layer Stall Inception," *Journal of Basic Engineering*, Series D, Vol. 83, No. 3, 1961, pp. 317–327.

[2]Sandborn, V. A., and Liu, C. Y., "On Turbulent Boundary Layer Separation," *Journal of Fluid Mechanics*, Vol. 23, No. 2, 1968, pp. 293–304.

[3]Sandborn, V. A., "Trends in Turbulent Boundary Layer Research," *Proceedings of the Third Engineering Mechanics Conference*, American Society of Civil Engineers, New York, 1979.

[4]Sandborn, V. A., and Seegmiller, H. L., "Evaluation of Mean and Turbulent Velocity Measurements in Subsonic Accelerated Boundary Layers," NASA TN D-8357, Nov. 1976.

[5]Sandborn, V. A., "Turbulent Boundary Layer Shear Pulses in Adverse Pressure Gradients," *Turbulence and Shear Flow-1*, edited by S. Banerjee and J. K. Eaton, Begell House, New York, 1999, pp. 1303–1308.

[6]Clauser, F. H., "Turbulent Boundary Layers in Adverse Pressure Gradients," *Journal of the Aeronautical Sciences*, Vol. 21, No. 2, 1954, pp. 91–108.

[7]Sandborn, V. A., "Equation for the Mean Velocity Distribution of Boundary Layers," NASA Memo 2-5-59E, Feb. 1959.

[8]Simpson, R. L., Chew, Y. T., and Shivaprasad, B. F., "Measurements of a Separating Boundary Layer," Office of Naval Research, Dept. of Navy, Project SQUID Rept. SMU4-PU; NTIS AD-A0952213, April 1980.

[9]Coles, D., "The Law of the Wake in the Turbulent Boundary Layer," *Journal of Fluid Mechanics*, Vol. 1, Pt. 2, 1954, pp. 191–226.

[10]Goradia, S. H., Mehta, J. M., and Shewsbury, G. S., "Analysis of the Separated Boundary Layer on the Surface and in the Wake of Blunt Trailing Edge Airfoils," NASA CR-145202, April 1977.

[11]Kline, S. J., Bardina, J. G., and Strawn, R. C., "Correlation of the Detachment of Two-Dimensional Turbulent Boundary Layers," *AIAA Journal*, Vol. 21, No. 1, 1983, pp. 68–73.

R. M. C. So
Associate Editor

Contribution to the Understanding of Flow Interactions Between Multiple Synthetic Jets

Mark Watson,* Artur J. Jaworski,† and Norman J. Wood‡
University of Manchester, Manchester, England M13 9PL, United Kingdom

Introduction

THE application of synthetic jet actuators (SJAs) for controlling flow behavior is gaining widespread acceptance. The vast majority of the work is being conducted in the area of aerospace, with the objective of modifying and manipulating separated flows over lifting surfaces. The fundamental physics of the flow generated by an SJA has been investigated experimentally by Smith and Glezer,[1] whereas numerical studies were conducted by Rizetta et al.[2]

In its most basic form, the SJA is a cavity that is bounded by an oscillating diaphragm on the bottom, whereas the top is covered by a rigid plate containing an orifice. Oscillations of the diaphragm cause the fluid to be alternately drawn into and expelled from the cavity in such a way that the net mass flow is zero. However, from the viewpoint of momentum or vorticity production, the effects of an SJA's operation are not neutral. A train of vortex rings, rolled up on the edge of the orifice, is formed, and it propagates outward from the orifice plate. Time-averaged velocity profiles in planes parallel to the orifice plate show a qualitative similarity with a steady jet, which explains the name "synthetic jet."

Early work on applications of SJAs was carried out by Smith et al.,[3] who utilized synthetic jets on a NACA airfoil and subsequently achieved a delay in the angle of stall from 5 to 18 deg. Wood et al.[4] reported a delay of the separation line associated with the flow past a circular cylinder. More recent work by Amitay and Glezer[5] showed that it is possible to manipulate the global aerodynamic forces on a thick airfoil, at high angles of attack, by deploying an array of SJAs with pulse-modulated actuation.

Received 25 July 2002; accepted for publication 18 August 2002.

*Research Student, School of Engineering, Oxford Road.

†Lecturer in Engineering, School of Engineering, Oxford Road; a.jaworski@man.ac.uk.

‡Professor of Aerospace Engineering, School of Engineering, Oxford Road. Senior Member AIAA.

Although the flow structures and flow behavior arising from isolated SJA devices seem to be well understood, in both the quiescent and crossflow conditions, the interaction between multiple synthetic jets has not been addressed with a sufficient level of detail. This problem is not trivial, and to date there are no design guidelines available as to the optimum spacing between the synthetic jets in an array for producing a desired aerodynamic effect. Moreover, application of synthetic jets on swept wings may lead to vortex trains interference and, thus, to combining or canceling the vorticity generated by the neighboring orifices. Further complications may arise if one wishes to modulate the relative phase lags between the excitation of devices forming an array.

This Note presents some preliminary flow visualizations that aim to explain the fundamental nature of such interactions between a pair of synthetic jets. The photographs of resulting smoke, ink, and surface flow visualizations are presented, and a discussion focused on explaining the flow phenomena is provided, together with suggestions for future research.

Experimental Setup

The experiments were conducted in three different situations: in still air inside a quiescent chamber, in the laminar crossflow of a water tunnel, and in a turbulent boundary layer in a wind tunnel. The setup for quiescent experiments was similar to that reported by Wood et al.[4] and consisted of a 50-mm-diam model of an SJA driven by an electromagnetic shaker at a frequency of 50 Hz. A number of orifice plates could be attached, each having two holes of diameter either 3.5 or 5 mm and a relative spacing between the holes of 6, 7, 8, 9, 10, 13, 16, and 20 mm. The exit velocity of the fluid was controlled by the level of excitation of the shaker and, for the results presented here, this was 5 m s^{-1}. Smoke was generated using a heated wire suspended inside the actuator cavity, along with mineral oil. A transverse cross section of the flow was visualized by a laser sheet obtained from a 5-W continuous argon ion laser.

The experiments in the laminar crossflow were conducted in a 10×14 in. water tunnel with a freestream velocity variable between 2 and 20 cm s^{-1}. A 100-mm shaker driven model of an SJA was mounted on a flat plate, which was submerged in the flow, and the same range of orifices was used. A food dye was used for visualizations, and two video cameras provided orthogonal views of the flow. The orifice plates could be rotated to vary the orifices' yaw angle relative to the freestream flow. The results presented here correspond to the diaphragm excitation frequency of 5 Hz, an exit velocity from the orifices of 8.5 cm s^{-1}, and a freestream velocity of 6.6 cm s^{-1}.

Finally, the experiments in the zero pressure gradient turbulent boundary layer were conducted in a 0.5×0.5 m low-speed wind tunnel operated at 32 m s^{-1}. Two small SJAs, similar to those described by Wood et al.[4] and Crook,[6] were mounted flush on a 0.5-m wide flat-plate airfoil, mounted in the tunnel center. The orifice diameters were 1 mm, whereas the spacing between orifices was 6 or 8 mm. The pair of SJAs were mounted within a metal disk, which could be rotated, allowing for variation in the yaw angle. The actuators were driven at a frequency of 1900 Hz, with the peak exit velocity from the orifice of 20 m s^{-1}. Surface visualizations of the flow were obtained by coating the airfoil with a mixture of kerosene and luminous paint and taking photographs with a digital camera.

Results and Discussion

Figure 1 shows the flow visualizations obtained for a pair of synthetic jets in quiescent conditions. The orifice plate is on the left in each of Figs. 1a–1c. The vortex structures are traveling from left to right. The only variable in the images shown in Fig. 1 is the spacing between orifices. Figures 1a–1c show that there are three types of interactions between synthetic jets.

For sufficiently large orifice spacing, the vortex rings from adjacent orifices seem to propagate unaffected by one another (Fig. 1a). When the distance between orifices is reduced (Fig. 1b), the roll up of the near side of each vortex ring, that is, the part of a ring nearest to an adjacent ring, gives rise to an induced velocity, acting on the opposite ring. This is a likely explanation for why the rings from